


## Article

# The Electric Vehicle Scheduling Problem for Buses in Networks with Multi-Port Charging Stations

Matina L. Y. Chau <sup>†</sup>, Diamanto Koutsompina <sup>†</sup> and Konstantinos Gkiotsalitis <sup>\*,†</sup> 

Department of Transportation Planning and Engineering, School of Civil Engineering, National Technical University of Athens, 15773 Athens, Greece; mchau@mail.ntua.gr (M.L.Y.C.); manto1811@gmail.com (D.K.)

\* Correspondence: kgkiotsalitis@civil.ntua.gr; Tel.: +30-21-0772-1286

<sup>†</sup> These authors contributed equally to this work.

**Abstract:** As more and more cities try to reduce their CO<sub>2</sub> emissions, public transport fleets are undergoing a transition from conventional to electric vehicles. To complete this shift, there is a need to build the required charging infrastructure. When the first electric buses were adopted, the charging stations were mostly built in the locations of large bus depots. However, in recent years, there has been a crowding problem in the charging stations resulting in queuing and unnecessary delays. In this study, we explore the potential of replacing single-port charging stations with multi-port charging stations that can serve multiple vehicles at once with a reduced charging rate. Because the charging rate reduces with the number of ports, we develop a mixed-integer linear program to determine the charging schedules of bus fleets in order to reduce the overall delays in the bus network. The novel formulation is tested in benchmark instances of various sizes demonstrating the improvement potential.

**Keywords:** electric bus scheduling; mixed-integer linear programming; public transport planning; branch and bound; charging infrastructure; transport electrification; EB-MDVSPTW



**Citation:** Chau, M.L.Y.; Koutsompina, D.; Gkiotsalitis, K. The Electric Vehicle Scheduling Problem for Buses in Networks with Multi-Port Charging Stations. *Sustainability* **2024**, *16*, 1305. <https://doi.org/10.3390/su16031305>

Academic Editors: Christina Iliopoulou and Konstantinos Kepaptsoglou

Received: 16 December 2023

Revised: 23 January 2024

Accepted: 30 January 2024

Published: 3 February 2024



**Copyright:** © 2024 by the authors. Licensee MDPI, Basel, Switzerland. This article is an open access article distributed under the terms and conditions of the Creative Commons Attribution (CC BY) license (<https://creativecommons.org/licenses/by/4.0/>).

## 1. Introduction

Preventative measures against global warming have been brought to the forefront in recent years, prioritizing the reduction of the overall use of fossil fuels. In addition to the environmental crisis, energy and fuel management have become all the more crucial due to supply-chain instability, perpetuated by COVID-19 and the rising political conflicts. Many countries have thus set out to explore opportunities to achieve stability and independence in terms of energy resource management, facilitated through the development of renewable energy sources. For instance, the European Commission's "REPowerEU" has outlined short-term measures to efficiently conserve energy, diversify energy supply, and accelerate the development of renewable energy resources to directly replace fossil fuels in buildings, industry, and the energy sector [1].

In terms of transportation, the reduction of CO<sub>2</sub> emissions can be achieved through the increase in Electric Vehicles (EVs) usage, supported by the heavy investment worldwide towards renewable energy resources. Given the current state of the mix of energy used however, CO<sub>2</sub> emissions are expected to continuously increase globally until 2035, despite the estimated 50% share of the adoption of EVs by then [2].

Generally, urban public transport is considered integral towards the development of sustainable transport, as it not only ensures the right to mobility for all residents, but also contributes to the conservation of energy and traffic decongestion, reducing travel time as a result. Low-cost public transport supports the shift in passenger demand from private cars to urban transit, ultimately leading to a reduced usage of private vehicles and consequently, mitigating their impact on the natural- and socio-economic urban environment.

Within public transport, buses are considered as "green" alternatives to private vehicles due to their potential to reduce greenhouse gas emissions per passenger [3,4]. Diesel

buses, however, are a source for concern over air pollution, particularly in urban areas. Instead, Electric Buses (EBs) are considered as the ideal technology due to their low- or zero emissions, energy efficiency, and near-silent operations [5]. Notwithstanding the above, diesel buses still outrank electric- or alternatively fueled buses in terms of usage [3,4]. As a result, the European Commission has proposed that by 2030, all new urban buses should be electric, aiming to reduce heavy-vehicle emissions in comparison to those of 2019 by 65% in 2035, and 90% in 2040 [1].

The continuously increasing volume of EBs in urban transport services worldwide further emphasizes the prevalence of EVs. The United States, for example, has had a rapid increase in the market share of EBs from a drastic 2% in 2007, to nearly 20% in 2015 [6]. The growing interest in EBs is reflected further in terms of the global EB market, which is expected to reach an evaluation of 215 billion by 2026, having experienced an annual growth rate of 26.1% throughout 2020 to 2026 [7]. Overall, research indicates that 30% of the global vehicle fleet for passengers will be electric by 2032. China is currently leading the adoption of EBs, with cities like Shenzhen replacing all heavy diesel buses with electric alternatives. In addition, the UK has deployed fleets of EBs in several cities, including London and Liverpool [8].

In terms of both planning and operations, the increase in EB use and its acceptance faces multiple challenges. The design of EB systems remains complex due to a variety of reasons, including energy and charging requirements, network design, as well as because of the necessary scheduling and planning, both based on the fixed charging stations [9]. The primary challenge lies within the low energy capacity of the vehicles' batteries, for which new recharging technologies have been proposed, like dynamic wireless power transfer, which extends the operational availability of EBs by charging the vehicles on the go. This method comes additionally at a lower cost to that of increasing battery size [10].

Inadequate charging infrastructure constitutes a major factor hindering the use of EBs and electric vehicles in general. This further solidifies the need for the development of new models that eliminate the disadvantages and drawbacks of the electrification of mobility, and in turn amplifies its benefits. In the area of Electric Vehicle Scheduling (E-VSP), the development of recovery methods supporting the practical implementation of EVs is considered as a direction for future research [11]. Integrated approaches to the scheduling of EBs have also received limited attention in past studies.

The operation of EBs requires frequent charging stops due to their limited autonomy. Given the usually restricted number of charging points in a network, this can result in significant charging delays, especially if the chargers are already occupied. With charging infrastructure already being established throughout multiple cities, along with the consistent growth of overall EV adoption, the high occupancy places EBs at an increased risk of facing difficulty for finding available charging stations [12].

A cost-effective solution to this would be the use of *multiple charging ports* within each charging point to enable the simultaneous charging of buses at the same location. Stations with multiple sockets facilitate charging to be shared between vehicles, offering increased scheduling flexibility to further manage delays at charging points. The design of charging ports is a vast topic of increased interest. Mukherjee and Sossan [13], for instance, developed a methodology to cost-optimally locate and size the design of a charging infrastructure for EVs within a power distribution grid. The notion of single- and multiple ports was accounted for and formulated, and it was determined that in comparison to alternative means, multi-port implementation is found to result in the lowest infrastructure costs, increasing driver flexibility and improving the arbitrating of charge. Such findings highlight the need for the thorough analysis of all facets of the design of charging infrastructure, and in this case, multi-port applications specifically. In considering the practical implementation of multi-port charging stations, relevant areas thus require continued investigation and should be examined in further detail to achieve the optimally efficient operation of electrically powered systems.

This paper will focus on the electric bus routing design problem in networks with fixed charging stations, equipped with *multiple ports* made available to each charger. In Section 2, this study presents the available literature on this field of research and identifies existing gaps in past literature. In Section 3, a new methodology for the Electric Bus Multiple-depot, Multi-Port Vehicle Scheduling Problem with Time Windows (EB-MDMPVSPTW) is presented. The applicability of the multi-port approach and new formulation is tested on a toy network, as well as on an additional set of ten different instances, used to analyze the computational performance of the method (Sections 4 and 5). Section 6 concludes the study and areas of further investigation will be suggested.

## 2. Literature Review

### 2.1. E-VSP: Electric-Vehicle Scheduling Problem

Electric-powered vehicles are purported as enablers of clean air initiatives, suitable for the design of sustainable solutions to reduce carbon and counter climate change [14]. This is particularly relevant for urban mobility, where EVs are considered as among the eco-friendliest means of transportation [15]. As a result, the management, testing, and design of batteries and their associated characteristics, like their state of charge, are prevalent topics of research as of late [14,15].

In considering the battery capacity of EVs, which typically ranges between 150 and 300 kWh [16], the long charging times, restricted driving ranges and the fixed charging stations, the electrification of vehicles could be considered well-suited for urban buses and their intrinsic characteristics. This is evident in the continued adoption of electric buses globally, spurring the scientific community to research solutions to the Electric-Vehicle Scheduling Problem (E-VSP), aiming for an improved and efficient management of public transportation.

Within the problem definition of the E-VSP, a set of scheduled trips need to be assigned to a set of electric vehicles with limited driving ranges, based on different depots, extending the Vehicle Scheduling Problem (VSP) [17–19]. The VSP is an established problem within the field of transport optimization, with several variations of it having emerged. Examples include the Multi-Vehicle Types VSP and the Alternative Fuel Vehicle Scheduling Problem (AF-VSP). For the AF-VSP, a heuristic construction approach was proposed by [20], alongside a column generation method. These algorithms were tested on the bus metropolitan system of Phoenix, Arizona.

Most studies have solved the E-VSP under near-ideal conditions, assuming for instance an unlimited supply of electrical energy and ignoring the risk of electricity load peaks, despite the two being significant parameters for electromobility. The start- and end time, and the start- and end location of the routes are all known in advance [17].

In the Electric Vehicle Scheduling Problem (E-VSP), each trip begins and ends at specific locations at predetermined times, and each vehicle can either be fully or partially recharged at any given charging station. The main objective is to use a small number of vehicles and to minimize the distance traveled between charging stations. How this problem extends specifically towards electric buses will be further determined in the next section.

### 2.2. EB-VSP: Electric Bus Vehicle Scheduling Problem

The purpose of this section is to review and evaluate existing methodologies on electric bus scheduling, which primarily focus on lowering costs and delays at charging stations.

Wen et al. [17] addressed the E-VSP for a set of bus routes, each of which starts and ends at specific locations and times. The routes must be operated by a set of electric buses or vehicles with driving range limits, each located at a restricted number of depots. The EBs may either be partially or fully charged at any of the specified charging stations. The objectives are to first minimize the number of vehicles required to cover all the scheduled journeys, and to then minimize the total travel distance. A mixed-integer programming formulation and an Adaptive Large Neighborhood Search (ALNS) heuristic method for the

EB-VSP were presented. ALNS was tested on a newly created set of EB-VSP benchmark instances. The results showed that the proposed heuristic can provide good solutions for solving EB-VSP in large networks, and optimal or near-optimal solutions when solving EB-VSP in small networks.

Rogge et al. [21] considered the constraints imposed by the range and charging time limitations of battery-powered buses. A methodology for the cost-optimized design of electric bus fleets and their corresponding charging station-based infrastructure was provided. The study used a genetic clustering algorithm, which included a mixed-integer linear programming formulation. The objective was to minimize the total cost of ownership of the entire bus system. The defined problem covered the scheduling of EBs, fleet composition, and the optimization of the charging infrastructure. The costs of vehicle schedule adjustments were calculated and evaluated along with the investment and operating costs of the bus system. The total cost of ownership allowed for the comparison of technical alternatives at the system level, which was particularly promising for studies investigating the feasibility of a vast range of technical approaches. Two European cities were analyzed as case studies, where it was concluded that the cost structure was significantly influenced by the considered bus types and their associated technical specifications. For example, the total energy consumption of the low-weight depot charging battery bus was up to 32% lower than the total consumption of the maximized battery capacity bus, despite the increased deadheading mileages. Conversely, the total costs of ownership for operating both bus types were relatively close, attributed to the increased fleet and driver costs necessary for light bus systems. The study also revealed that a mixed fleet of different bus types could be beneficial depending on the operational characteristics of the bus route.

A mixed-integer linear programming model for optimizing electric bus charging schedules was developed by [22], where both scheduling and operational decisions were determined, while minimizing the total annual cost. The results showed that the problem of limited bus autonomy can be alleviated by adopting certain charging strategies. The analyses demonstrated that the model was capable of providing transportation services with comprehensive guidance on the use of electric buses, as well as the development of fast-charging systems. The comparative results indicated that it was more economical and environmentally friendly to use electric buses than diesel-powered buses.

In 2018, Jiang et al. [23] studied the scheduling of electric buses under regular charging conditions in Shenzhen, a large city based in southern China. The aim was to create routing schedules and charging plans for EBs based on their given timetables, minimizing the overall operating costs. Described as a vehicle scheduling problem with multiple depots, the charging demands of EBs were considered. To solve the problem, a neighbourhood search-based heuristic with a charging and bus allocation policy was proposed. According to the scenario of this study, the algorithm was developed for trunk bus operations, characterized by short time intervals and long travel distances. It is also applicable however to the optimization of other types of bus routes.

Yao et al. [24] proposed a new methodology for the E-VRP with multiple vehicle types in public transportation, based on a given multi-vehicle schedule. The differences in driving range, charge-duration, and energy consumption of the electric buses for multiple vehicle types were considered, formulating an optimization model created to minimize the total annual scheduling cost, including the purchasing cost of electric buses and chargers, the operating cost of deadheading, and the scheduled routes. Based on the charging route, a heuristic procedure was then developed to find the optimal solution. The research was validated through the use of a real transport network in the Daxing district of Beijing. The optimized results provided transportation agencies with guidance on the purchasing and scheduling of electric buses for multiple vehicle types, as well as for the deployment of chargers. The comparative analysis showed that the proposed method accounted for the replacements between electric vehicle types, reducing the annual total scheduling cost by 15.93%.

Li et al. [25] focused on the development of a joint model to optimize the scheduling of a regular electric bus transit charging network under fixed charger deployment. The policy of partial charging and electricity prices during the time of usage were considered. The model set out to minimize the total investment cost of the transit system, including capital and maintenance costs of the electric buses and chargers, energy consumption costs, and costs associated with operating time. A solution procedure based on the improved adaptive genetic algorithm was followed and the model was validated using a transit network in the Anting Town of Shanghai, comprised of eight individual bus lines and 867 daily trips. The results demonstrated that the consideration of the partial charging policy tailors the charging schedule to the electricity prices during the usage period. Compared to the benchmark of the separate scheduling for each line, the proposed model is capable of yielding investment savings with the high usage of electric buses and battery chargers.

Liu and Ceder [26] considered the scheduling problem of battery-powered electric transit vehicles with stationary chargers installed at transit terminals. Two equivalent mathematical formulations of the problem were provided. The first was based on the theory of the deficit function, and the second was an equivalent bi-objective integer programming model. The first objective was to minimize the required total number of electric vehicles, while the second was to minimize the total number of necessary chargers. To solve the bi-objective Battery-Electric Transit VSP (BET-VSP), two solution methods were developed. A lexicographic-based solution procedure consisting of the two stages of construction and optimization was proposed. A customized maximum flow solution method was then developed. Three numerical examples were used to illustrate the application of the solution methods, along with a real-world case study in Singapore. The results demonstrated that the proposed framework and solution methods were effective, solidifying the potential for the methodologies' real-world application of solving the scheduling problem for large-scale BET-VSP of electric transit vehicles with fixed chargers installed at transit terminals.

Zhang et al. [27] studied the long-term strategies of bus electrification, optimizing the development of charging infrastructure and bus fleet in parallel. Seasonal differences related to battery capacities, bus routes and schedules were accounted for in the modeling phase. A mixed-integer linear program determining detailed charging schedules was formulated, specifying the charging locations and times, aiming to minimize both costs and emissions. Tested on a real case study, the computational results showed that replacing diesel-powered buses with EBs saved 17.8% of the total cost and reduced 39.3% of carbon emissions. Compared to designing a period-by-period plan, the implementation of long-term bus electrification was capable of saving 13.5% of total costs, and 21.7% of operating costs specifically. Moreover, the benefits of long-term EB implementation grew in significance for a longer planning horizon.

Montoya et al. [28] extended existing E-VRP models to consider nonlinear charging functions. Most E-VRP models assumed the battery charge level to be a linear function of charging time, when in reality the function is nonlinear. A hybrid metaheuristic method combining elements from the literature with those designed specifically for this problem was created. The method was used to evaluate the importance of nonlinear charging functions. A computational study was presented to compare the common assumptions of previous literature with those that were proposed in this study. Findings indicated that the neglect of nonlinear charging can result in infeasible or excessively costly solutions. The hybrid metaheuristic was also tested on a set of 120 instances, for which the method was found to perform well.

Felipe et al. [29] addressed a variant of the vehicle routing problem of a fleet consisting of electric vehicles with limited autonomy. This problem considered the possibility of performing partial charging, as well as the use of different charging technologies, potentially capable of saving additional costs and energy. A mathematical programming model was presented which could only be optimally solved for very small cases. Hence, several heuristic algorithms were considered to solve real-size instances. Extensive computational



results examining a variety of cases were reported, evaluating the performance of the proposed algorithms, and analyzing the distinct features inherent to the problem (such as size, geographical configuration, charging stations, autonomy, technologies and more).

Recently, Gkiotsalitis et al. [30] extended the Multi-Depot Vehicle Scheduling Problem with Time Windows (MDVSPTW) to the case of electric vehicles capable of charging at any existing set of charging stations located within the service area. A mixed-integer nonlinear formulation (MINLP) was developed for the electric bus multi-depot vehicle scheduling problem with time windows (EB-MDVSPTW). The model covered the operating cost of the buses, vehicle waiting times and charging station capacity. The simultaneous charging of different vehicles at the same charger was prohibited. Chargers were modeled as task nodes of an extended network and could be placed at any location based on a city's existing charging infrastructure, rather than only using chargers dedicated to EBs. Furthermore, the EB-MDVSPTW MINLP was linearised, reformulated into a mixed-integer linear model (MILP). The solution space was restricted by the introduction of valid inequalities, which were evaluated through computational experiments.

To conclude this literature review, the papers relevant to the scope of the EB-VSP and their associated contributions are summarized in Table 1.

**Table 1.** Summary of relevant past studies.

Study	Objectives	Problem	Mathematical Model	Solution Method
[17]	Minimization of the number of required vehicles and the total travel distance	Define the schedules of electric buses and charging	Mixed integer program	Metaheuristic–Adaptive Large Neighborhood Search
[21]	Minimize the total cost of ownership of EV fleets	Scheduling of EBs and their chargers and fleet composition	Mixed integer linear program	Metaheuristic–Genetic Algorithm
[22]	Minimize the annual total EB recharging system operating costs	Rescheduling of the charging timeplans of electric buses	Mixed integer linear program	Exact (CPLEX solver)
[23]	Minimize the total operational costs	Define the charging plans and electric bus schedules	No formulation	Neighborhood Search Based Heuristic
[24]	Minimize the annual total scheduling costs including purchasing and operating costs	EB type scheduling considering chargers used	Integer Program	Metaheuristic–Genetic Algorithm
[25]	Minimize the total investment cost including capital and maintenance cost of EBs and chargers, the power consumption cost, and time-related in-service cost	EB scheduling and stationary charger deployment considering partial charging policy and time-of-use electricity prices	Mixed-integer Program	Metaheuristic–Genetic Algorithm
[26]	Minimize the required number of electric buses and charging stations	Define the vehicleschedules of EBs considering limited range and charging requirements	Bi-objective Integer Programming	Lexicographic Method
[28]	Minimize the total time (travel, detour and charging times)	Electric bus schedules, considering a nonlinear function of the charging times	Mixed integer linear program	Metaheuristic–Iterated Local Search and Heuristic Construction
[29]	Minimization of the total recharging cost	Electric bus scheduling, considering the possibility of partial recharging	Integer Program	Heuristics–greedy generation method (k-PseudoGreedy) and Simulated Annealing

Table 1. Cont.

Study	Objectives	Problem	Mathematical Model	Solution Method
[30]	Minimize the total cost of operations	Define the electric bus schedules and the charging schedules	Mixed integer linear program	Exact (Gurobi solver)
[27]	Minimize the total cost of operations and emissions	Define the charging schedules	Mixed integer linear program	Exact (CPLEX solver)

The overview of the most relevant past studies in Table 1 underlines the extensive literature of the EB-VSP problem with respect to scheduling the assignment of electric buses to trips and the scheduling of their charging times. The reviewed studies, however, do not consider the use of multiple ports at the same charging station and the potential charging rate reductions when several ports are used at the same time. Thus, this study sets out to directly extend the EB-VSP problem to the case of multi-port charging stations. Departing from the traditional EB-VSP problem with Time Windows presented in [30], the contribution of our study lies in the remodeling of the EB-VSP to account for multi-port charging events with varying charging rates. Our model is then tested on a toy network and a set of benchmark instances, remodeled to consider multi-port charging infrastructure.

### 3. Methodology

We expand the Single-Port, Electric Bus Multiple-depot Vehicle Scheduling Problem in Time Windows (EB-MDVSPTW) to the Multi-port EB-MDVSPTW, where two or more ports can be placed at the same charging station providing the opportunity to charge multiple buses simultaneously at the same spot. The obvious advantage is that if a charging station location is beneficial to some bus lines (i.e., it is in close proximity to the lines' terminal), multiple buses from these lines can charge there using several ports, instead of traveling to a distant charging station location. Notwithstanding this, if multiple ports of a charging station are used at the same time, the charging rate reduces because the power supply of a charging station is divided among multiple ports. In comparison, single port energy consumption is fixed, and with increased vehicle usage, due to the fixed energy consumption of the single-ports, the rate of energy use increases significantly more than that of the multi-port infrastructure, which may not be sustainable for the power grid. To support the sustainable use of the multi-port variant, which yields slower charging, a trade-off emerges for bus drivers: visit charging stations in close proximity which have some of their ports occupied resulting in slower charging or visit unoccupied charging stations which are far away and require higher deadheading times?

In this study, we formulate the Multi-port EB-MDVSPTW by building upon the single-port EB-MDVSPTW formulation developed by [30]. Let us consider that each vehicle  $k$  starts from its depot and returns to the same depot at the end of its daily schedule. The locations of the charging stations are pre-defined during the strategic planning phase of the electric bus network design problem [31], and they might have been placed at any point in the network, even at the locations of the depots.

We consider a set of  $Z = \{1, \dots, z, \dots\}$  charging stations in our bus network. The bus network as a number of pre-scheduled trips, which, together with the charging events, can be modeled as tasks that must be performed by vehicles. We note that, unlike tasks that refer to pre-scheduled trips, the number of charging requests per charging station is not fixed because it depends on the assignment of electric buses to charging stations. We consider that (1) all EBs are fully charged at the beginning of the day; (2) charging infrastructure can be shared among different EBs; (3) all installed chargers have the same charging supply rate; and (4) EBs recharge fully when plugged in a charging station. In addition, when we use multiple ports of a charging station, its charging supply rate per vehicle drops because it needs to accommodate multiple requests.

Let  $F$  be the set of all possible charging events. Each possible charging event  $i \in F$  can start within the time window  $[l_i, u_i]$ . Charging events  $i \in F$ , associated with charger  $z \in Z$ , form a subset  $F^z \subseteq F$ . Each possible charging event  $i \in F$  can be seen as an additional node in the network of a vehicle  $k \in K$  that comprises the following nodes:

$$N^k = \{V^k \cup F \cup \{o_k, d_k\}\}$$

where  $V^k \subseteq V$  are the trips that can be potentially performed by vehicle  $k$  and are a subset of set  $V$  denoting all trips,  $(o_k, d_k)$  the origin and destination depots of trip  $k$ , and  $F$  the set of all charging events. The set of all nodes that are available to all vehicles is:

$$N = \{V \cup F \cup O \cup D\}$$

where  $O$  and  $D$  are the sets of the origin and destination depots for all vehicles. Network  $G^k$  can be expressed as:

$$G^k = (N^k, A^k)$$

where arcs  $A^k$  are the union of the following sets:

$$A^k = \begin{cases} A_1^k = (o_k, j) \quad \forall j \in N^k - \{o_k\} \\ A_2^k = (j, d_k) \quad \forall j \in N^k - \{o_k, d_k\} \\ A_3^k = (i, j) \quad \forall i \in V^k \quad \forall j \in V^k - \{i\} \\ A_4^k = (i, j) \quad \forall i \in V^k \quad \forall j \in F \\ A_5^k = (i, j) \quad \forall i \in F \quad \forall j \in V^k \end{cases}$$

For vehicle  $k \in K$ , arcs  $A_1^k$  are all feasible arcs that start from the origin depot,  $A_2^k$  are all feasible arcs that connect a node to the destination depot,  $A_3^k$  are all feasible arcs which represent the traveling from the end location of trip  $i \in V^k$  to the start location of trip  $j \in V^k - \{i\}$ ,  $A_4^k$  are all feasible arcs which represent the traveling from the end location of trip  $i$  to the location of the charging event  $j \in F$ , and arcs  $A_5^k$  are all feasible arcs which represent the traveling from the location of charging event  $i \in F$  to the start location of trip  $j$ .

Every node has a vehicle-independent lower and upper time bound of starting the task associated with it. This is expressed by  $[l_i, u_i]$ , where  $l_i$  is the lower bound and  $u_i$  is the upper bound of every node  $i \in N$ . In addition, to complete any trip  $i \in V$  there is an associated time cost  $\tilde{t}_i$ ,  $\forall i \in V$ . To travel from the end location of the task at node  $i \in N$  to the start location of the task at node  $j \in N$  there is an associated travel cost  $t_{ij}$ .

The nomenclature of the multi-port EB-MDVSPTW problem is provided in Table 2.

Each vehicle  $k \in K$  starts its operations fully charged with a SOC  $\phi_{max}^k$ . Given the number of ports  $\psi_i$  used at the charging event  $i \in F$ , a vehicle  $k$  which arrives at a charging node at time  $T_i^k$  with a current energy level of  $e_i^k$  and needs to recharge fully, it will require a time period:

$$\tau_i^k = (\phi_{max}^k - e_i^k) / r_i \quad (1)$$

to fully recharge. That is, vehicle  $k$  can move to the next node after time  $T_i^k + \tau_i^k$ .

The SOC of every vehicle  $k$  at the beginning of its daily operations is the maximum possible. That is,  $\bar{e}_{o_k}^k = \phi_{max}^k$ , where  $\bar{e}_{o_k}^k$  is the SOC of vehicle  $k$  when departing from node  $o_k$ . Given the SOC when vehicle  $k$  arrives at node  $i \in V^k \cup F$ ,  $e_i^k$ , and when it completes its task at that node,  $\bar{e}_i^k$ , we have that:

$$\bar{e}_i^k = e_i^k - g_i^k \quad (2)$$



where  $g_i^k$  is the vehicle's SOC change when performing task  $i$ . If task  $i \in V^k$ , then vehicle  $k$  performs trip  $i$  and it consumes energy  $\eta_i \geq 0$ . If, however,  $i \in F$ , then  $g_i^k = e_i^k - \phi_{max}^k$  because the vehicle will recharge up to its maximum allowed SOC.

**Table 2.** EB-MDVSPTW nomenclature.

Notation:	
Sets:	
$K$	set of available vehicles
$Z$	set of charging stations
$O, D$	sets of origin and destination depots
$V$	set of trips
$V^k$	subset of scheduled trips that can be accomplished by vehicle $k$
$F$	set of all possible charging events
$F_0$	$F_0 \subseteq F$ is the set of all possible charging events after removing the latest possible charging events at every charger
$F^z$	subset of possible charging events at charger $z \in Z$ ordered from the first to the last
$N^k$	subset of nodes associated with vehicle $k$ , $V^k \cup F \cup \{o_k, d_k\}$
$N$	set of all possible task nodes, $N = \{V \cup F \cup O \cup D\}$
$A^k$	set of feasible arcs for vehicle $k \in K$
$G^k$	$G^k = (N^k, A^k)$ is the network associated with vehicle $k$
Parameters:	
$r_j$	charging rate associated with charging event $j \in F$
$\psi_j$	number of ports used at charging event $j \in F$
$\xi_z$	number of ports available at each charging station $z \in Z$
$o_k, d_k$	the source node and the sink node associated with the depot housing vehicle $k$
$[l_i, u_i]$	time window associated with each node $i \in N$
$t_{i,j}$	elapsed time on arc $(i, j)$ which is equal to the travel time between the end location of task $i \in N$ and the start location of task $j \in N$
$\tilde{t}_i$	required travel time to conduct trip $i \in V$
$\lambda$	unit waiting cost of a vehicle
$b_{ij}^k$	the cost constant component of performing task $j$ after task $i$ without considering any potential delay (task $j$ starts immediately after $i$ without time delays).
$\phi_{max}^k$	SOC of vehicle $k$ when it is fully charged
$\phi_{min}^k$	minimum allowed SOC level for vehicle $k$
$\eta_i$	consumed energy when performing trip $i \in V$
$\theta_{ij}$	consumed energy when deadheading from the end location of node $i \in N$ to the start location of node $j \in N$
$M$	a very large positive number
$q_j$	vector $q : V \rightarrow F$ returns the closest charging event location $q_j \in F$ to the end location of trip $j \in V$
$\omega_i$	vector that returns the next charging event of charging event $i$ that is performed at the same charging station
Variables:	
$e_i^k$	SOC of vehicle $k$ when it arrives at node $i \in V^k \cup F \cup \{d_k\}$
$\bar{e}_i^k$	SOC of vehicle $k$ when it completes the task at node $i \in V^k \cup F \cup \{o_k\}$
$\tau_i^k$	required time period to recharge vehicle $k$ via charging event $i \in F$
$g_i^k$	vehicle SOC change when performing task $i \in V^k \cup F$
$x_{ij}^k$	binary flow variables, where $x_{ij}^k = 1$ if vehicle $k$ uses arc $(i, j) \in A_k$ and 0 otherwise
$y_i^k$	binary indicator variables, where $y_i^k = 1$ if charging event $i \in F$ is performed by vehicle $k$ and 0 otherwise
$T_i^k$	time that service begins at node $i \in N^k$ . $T_{o_k}^k$ indicates the departure time from the depot, $T_{d_k}^k$ the arrival time at the depot, and $T_i^k$ the time that service begins at any other node $i \in V^k \cup F$

Expanding the EB-MDVSPTW formulation of [30] to the case of multiple ports, the **vehicle scheduling constraints** are now reformulated as follows:

$$\sum_{k \in K} \sum_{i:(i,j) \in A_k} x_{ij}^k = 1 \quad \forall j \in V \quad (3)$$

$$\sum_{k \in K} \sum_{i:(i,j) \in A_k} x_{ij}^k \leq \psi_j \quad \forall j \in F \quad (4)$$

$$\sum_{j:(o_k,j) \in A^k} x_{o_k,j}^k = \sum_{i:(i,d_k) \in A^k} x_{i,d_k}^k = 1 \quad \forall k \in K \quad (5)$$

$$\sum_{i:(i,j) \in A^k} x_{ij}^k - \sum_{i:(j,i) \in A^k} x_{ji}^k = 0 \quad \forall k \in K \quad \forall j \in V^k \cup F \quad (6)$$

$$x_{ij}^k (T_i^k + \bar{t}_i + t_{ij}) \leq x_{ij}^k T_j^k \quad \forall k \in K \quad \forall (i,j) \in A^k \mid i \in V^k \quad (7)$$

$$x_{o_k,j}^k (T_{o_k}^k + t_{o_k,j}) \leq x_{o_k,j}^k T_j^k \quad \forall k \in K \quad \forall (o_k,j) \in A^k \quad (8)$$

$$x_{ij}^k (T_i^k + \tau_i^k + t_{ij}) \leq x_{ij}^k T_j^k \quad \forall k \in K \quad \forall (i,j) \in A^k \mid i \in F \quad (9)$$

$$\tau_i^k = (\phi_{max}^k - e_i^k) / r_i \quad \forall i \in F \quad \forall k \in K \quad (10)$$

$$l_i \leq T_i^k \leq u_i \quad \forall k \in K \quad \forall i \in N^k \quad (11)$$

$$x_{ij}^k \in \{0, 1\} \quad \forall k \in K \quad \forall (i,j) \in A^k \quad (12)$$

These constraints include several amendments compared to the MDVSPTW formulation. Constraints (3) ensure that each trip  $j \in V$  will be performed by exactly one vehicle. Constraints (4) ensure that a charging event  $j \in F$  can be utilized at most  $\psi_j$  times, where  $\psi_j$  is the number of ports in use in this charging event and is an additional feature of the multi-port formulation. Constraints (5) ensure that each vehicle  $k \in K$  will start from its origin depot and return to its destination depot. Constraints (6) consider the charging events in the network's constraints related to the conservation of flow. Constraints (7) do not consider arcs that have nodes from set  $F$  as their origin nodes because the elapsed travel time between activities  $(i,j)$  does not depend on  $t_{ij}$ . Constraints (8) ensure that if vehicle  $k$  departs from its depot  $o_k$  and moves to  $j$ , then the departure time from the depot,  $T_{o_k}^k$ , plus the required time to travel from  $o_k$  to  $j$  is less than or equal to the time that service begins at node  $j$ . We introduce constraints (9) where  $i$  is a charging event  $i \in F$  and the elapsed time on arc  $(i,j)$  is equal to the duration of task  $i$ ,  $\tau_i^k$ , plus the travel time between the end location of task  $i$  and the start location of task  $j$ ,  $t_{ij}$ . Constraints (10) return the values of  $\tau_i^k$ , considering the charging rate changes when multiple ports are in use. Constraints (11) ensure that the activity at each node  $i$  starts within its time window  $[l_i, u_i]$ . Finally, constraints (12) ensure that each arc  $(i,j)$  can be traversed by vehicle  $k$  or not.

In addition to the vehicle scheduling constraints, we have the additional electric charging constraints related to the charging scheduling and the state of charge of EBs. Operating arc  $(i,j) \in A^k$  is permitted if, and only if,

$$e_j^k \geq \phi_{min}^k \quad (13)$$

where  $e_j^k \geq \phi_{min}^k$  ensures that the SOC of vehicle  $k$  is sufficient when arriving at node  $j$ . The **electric charging constraints** are:

$$e_{o_k}^k = \phi_{max}^k \quad \forall k \in K \quad (14)$$

$$e_j^k = e_j^k - g_j^k \quad \forall j \in V^k \cup F, \quad \forall k \in K \quad (15)$$

$$e_j^k \geq (e_i^k - \theta_{ij}) x_{ij}^k \quad \forall (i,j) \in A^k, \quad \forall k \in K \quad (16)$$

$$e_j^k \leq (e_i^k - \theta_{ij}) + (1 - x_{ij}^k) M \quad \forall (i,j) \in A^k, \quad \forall k \in K \quad (17)$$

$$g_i^k = \eta_i \quad \forall i \in V^k \quad \forall k \in K \quad (18)$$

$$g_i^k = e_i^k - \phi_{max}^k \quad \forall i \in F \quad \forall k \in K \quad (19)$$

$$\phi_{min}^k \leq e_j^k \quad \forall k \in K \quad \forall i \in V^k \cup F \cup \{d_k\} \quad (20)$$

$$y_i^k = \sum_{j:(i,j) \in A_k} x_{ij}^k \quad \forall i \in F \quad \forall k \in K \quad (21)$$

$$\sum_{k \in K} y_i^k (T_i^k + \tau_i^k) \leq T_{\omega_i}^k + M(1 - \sum_{\rho: (\omega_i, \rho) \in A^k} x_{\omega_i \rho}^k) \quad \forall i \in F_0, \quad \forall k \in K \quad (22)$$

Constraints (14)–(19) return the SOC values when vehicles are traveling between nodes. Notice that when  $x_{ij}^k = 1$  constraints (16) and (17) force  $e_j^k$  to be equal to the SOC value after departing from node  $i$ ,  $\bar{e}_i^k$ , minus the consumed energy to travel from  $i$  to  $j$ ,  $\theta_{ij}$  (the proof is provided in [30]).

Constraints (20) ensure that the SOC of vehicle  $k$  when arriving at node  $j \in V^k \cup F \cup \{d_k\}$  is greater than or equal to the minimum allowed SOC limit. Finally, constraints (21) and (22) ensure that if a charging port is used by a vehicle during charging event  $i \in F$ , the next charging event at the same charging port, denoted as  $\omega_i$ , will start after the end time of the charging event at this port. This does not allow two vehicles to use the same charging port simultaneously.

The EB-MDVSPTW is a mixed-integer nonlinear program (MINLP) with nonlinear objective function and nonlinear constraints (7)–(9), (16) and (22). That is, even if we relax the integralities of the binary variables, we still need to solve a nonlinear program with several nonlinear constraints. This can be achieved by adopting the reformulation of [30] which linearizes the nonlinear constraints. Namely, constraints (7)–(9) can be linearized by replacing them with the equisatisfiable linear constraints (23)–(27):

$$T_i^k + \bar{t}_i + t_{ij} - T_j^k + \sigma_{ij}^k \leq 0 \quad \forall k \in K \quad \forall (i, j) \in A^k \mid i \in V^k \quad (23)$$

$$T_{o_k}^k + t_{o_k j} - T_j^k + \sigma_{o_k j}^k \leq 0 \quad \forall k \in K \quad \forall (o_k, j) \in A^k \quad (24)$$

$$T_i^k + \tau_i^k + t_{ij} - T_j^k + \sigma_{ij}^k \leq 0 \quad \forall k \in K \quad \forall (i, j) \in A^k \mid i \in F \quad (25)$$

$$\sigma_{ij}^k \leq M(1 - x_{ij}^k) \quad \forall k \in K \quad \forall (i, j) \in A^k \quad (26)$$

$$\sigma_{ij}^k \geq -M(1 - x_{ij}^k) \quad \forall k \in K \quad \forall (i, j) \in A^k \quad (27)$$

where  $\sigma_{ij}^k \in \mathbb{R}$  for  $(i, j) \in A^k, k \in K$  are continuous variables.

In addition, the nonlinear constraints (16) can be replaced by the following equisatisfiable set of linear inequality constraints (28)–(30), where  $\bar{\sigma}_{ij}^k$  are newly introduced continuous variables:

$$e_j^k \geq (\bar{e}_i^k - \theta_{ij}) + \bar{\sigma}_{ij}^k \quad \forall (i, j) \in A^k, \quad \forall k \in K \quad (28)$$

$$\bar{\sigma}_{ij}^k \leq M(1 - x_{ij}^k) \quad \forall (i, j) \in A^k, \quad \forall k \in K \quad (29)$$

$$\bar{\sigma}_{ij}^k \geq -M(1 - x_{ij}^k) \quad \forall (i, j) \in A^k, \quad \forall k \in K \quad (30)$$

Finally, nonlinear constraints (22):

$$\sum_{k \in K} y_i^k (T_i^k + \tau_i^k) \leq T_{\omega_i}^k + M(1 - \sum_{\rho: (\omega_i, \rho) \in A^k} x_{\omega_i \rho}^k) \quad \forall i \in F_0, \quad \forall k \in K$$

can be linearized into (31)–(33) by adding continuous variables  $\tilde{\sigma}_i^{k_0}$  for all  $i \in F$  and  $k_0 \in K$  (see proof in [30]):

$$T_i^{k_0} + \tau_i^{k_0} + \tilde{\sigma}_i^{k_0} \leq T_{\omega_i}^k + M(1 - \sum_{\rho: (\omega_i, \rho) \in A^k} x_{\omega_i \rho}^k) \quad \forall i \in F_0 \quad \forall k \in K \quad \forall k_0 \in K \quad (31)$$

$$\tilde{\sigma}_i^{k_0} \leq M(1 - y_i^{k_0}) \quad \forall i \in F_0 \quad \forall k_0 \in K \quad (32)$$

$$\tilde{\sigma}_i^{k_0} \geq -M(1 - y_i^{k_0}) \quad \forall i \in F_0 \quad \forall k_0 \in K \quad (33)$$

Finally, consider the nonlinear objective function:

$$\begin{aligned} \min \quad & \sum_{k \in K} \sum_{(i,j) \in A_k \mid i \in V^k} \left( b_{ij}^k + \lambda(T_j^k - T_i^k - \tilde{t}_i - t_{ij}) \right) x_{ij}^k + \\ & \sum_{k \in K} \sum_{(i,j) \in A_k \mid i \in F} \left( b_{ij}^k + \lambda(T_j^k - T_i^k - \tau_i^k - t_{ij}) \right) x_{ij}^k \end{aligned}$$

To linearize it, one can introduce continuous variables  $z_{ij}^k$  that take the value of:

- $\left( b_{ij}^k + \lambda(T_j^k - T_i^k - \tilde{t}_i - t_{ij}) \right) x_{ij}^k$  for  $(i, j) \in A_k \mid i \in V^k$
- and  $\left( b_{ij}^k + \lambda(T_j^k - T_i^k - \tau_i^k - t_{ij}) \right) x_{ij}^k$  for  $(i, j) \in A_k \mid i \in F$

This is enforced by the following set of linear inequality constraints (34)–(39):

$$z_{ij}^k \leq x_{ij}^k M \quad \forall k \in K, (i, j) \in A_k \mid i \in V^k \cup F \quad (34)$$

$$z_{ij}^k \geq -x_{ij}^k M \quad \forall k \in K, (i, j) \in A_k \mid i \in V^k \cup F \quad (35)$$

$$z_{ij}^k \leq b_{ij}^k + \lambda(T_j^k - T_i^k - \tilde{t}_i - t_{ij}) + M(1 - x_{ij}^k) \quad \forall k \in K, (i, j) \in A_k \mid i \in V^k \quad (36)$$

$$z_{ij}^k \leq b_{ij}^k + \lambda(T_j^k - T_i^k - \tau_i^k - t_{ij}) + M(1 - x_{ij}^k) \quad \forall k \in K, (i, j) \in A_k \mid i \in F \quad (37)$$

$$z_{ij}^k \geq b_{ij}^k + \lambda(T_j^k - T_i^k - \tilde{t}_i - t_{ij}) - (1 - x_{ij}^k) M \quad \forall k \in K, (i, j) \in A_k \mid i \in V^k \quad (38)$$

$$z_{ij}^k \geq b_{ij}^k + \lambda(T_j^k - T_i^k - \tau_i^k - t_{ij}) - (1 - x_{ij}^k) M \quad \forall k \in K, (i, j) \in A_k \mid i \in F \quad (39)$$

and the objective function is then replaced by:

$$\min \quad \sum_{k \in K} \sum_{(i,j) \in A_k \mid i \in V^k \cup F} z_{ij}^k \quad (40)$$

Using the aforementioned linearizations, the multi-port EB-MDVSPTW problem becomes a mixed-integer linear program that can be solved to global optimality with branch and bound. Notwithstanding this, the multi-depot EB-MDVSPTW is NP-Hard as the extension of the exact cover problem (see proof in [30]), meaning that we can solve it to global optimality for medium-sized problem instances.

#### 4. Case Study

##### Multi-Port Toy Network Demonstration

The application of the proposed formulation was demonstrated on a toy network, designed as small in scale to clearly present and detail the model's input and associated output, supporting reproducibility. Two electric bus lines (consisting of two vehicles  $K = \{1, 2\}$ ) were considered for the network, each vehicle performing a total of three trips. The first line's set of trips starts at depot  $o_1$  with the respective latitude and longitude coordinates (677908, 6150220) of the geographic coordinate system. The EB then returns to the coordinates (585053, 6140355) of depot  $d_1$ . The second EB starts from the coordinates (677908, 6150220) of depot  $o_2$  and finishes its trip at depot  $d_2$  with coordinates (720134, 6210199). It should be noted that origin depots  $o_1$  and  $o_2$  share the same physical location, whereas the destination depots  $d_1$  and  $d_2$  are located differently. The toy network consists of two charging stations  $Z = \{1, 2\}$ , producing a set

of 16 charging events  $F = \{1001, 1011, 1021, 1031, 1002, 1012, 1022, 1032, 2001, 2011, 2021, 2031, 2002, 2012, 2022, 2032\}$ . The charging event indexing uses the conventions presented in Table 3.

**Table 3.** Explanation of the indexing of multi-port charging events.

Description	No. of Ports Used	-	Time Sequence Interval $0 \rightarrow 1 \rightarrow 2 \rightarrow 3$	Charging Station Z
e.g., charging event explanation	1	0	1	2
	1 port is used		Time interval 1, which is after 0	Charging station 2
e.g., charging event explanation	2	0	2	1
	2 ports are used		Time interval 2, which is after 1	Charging station 1

Charging events 1001 and 2011 are for example both performed at charging station  $Z = 1$ , and charging events 1022 and 2002 at charging station  $Z = 2$ . Charging events 1031, 2031, 1032 and 2032, indexed by 3, represent the final instances of the charging event sequence. Should there be a change in the number of ports used, the event is then represented as next in the sequence interval. For instance, should a vehicle leave charging station  $Z = 1$  when two ports are currently occupied, then the charging event switches from 2011 to 1021, representing the occupation of only one port. Should a vehicle join charging station  $Z = 2$  when one port is already occupied and another is available, then the event index changes from 1002 to 2012, representing dual-port charging. The complete set of task nodes  $N$  consists of:

$$N = \{o_1, o_2, 1, 2, 3, 4, 5, 6, d_1, d_2, 1001, 1011, 1021, 1031, 1002, 1012, 1022, 1032, 2001, 2011, 2021, 2031, 2002, 2012, 2022, 2032\}$$

and the set of trips  $V = \{1, 2, 3, 4, 5, 6\}$ .

Each vehicle is allowed to theoretically perform any trip, thus  $V^k = 1 = V^k = 2 = \{1, 2, 3, 4, 5, 6\}$  and Task nodes  $N^k = 1$  of vehicle 1 and  $N^k = 2$  of vehicle 2 are as follows:

$$N^1 = \{o_1, 1, 2, 3, 4, 5, 6, d_1, 1001, 1011, 1021, 1031, 1002, 1012, 1022, 1032, 2001, 2011, 2021, 2031, 2002, 2012, 2022, 2032\}$$

and

$$N^2 = \{o_2, 1, 2, 3, 4, 5, 6, d_2, 1001, 1011, 1021, 1031, 1002, 1012, 1022, 1032, 2001, 2011, 2021, 2031, 2002, 2012, 2022, 2032\}$$

The geographical coordinates of all task nodes  $N$  are presented in Table 4. Note that the trip nodes  $V = \{1, 2, 3, 4, 5, 6\}$  have different origin and destination locations, representing the first and last stop of the trip, whereas depot nodes  $o_1, o_2, d_1, d_2$  and charging event nodes  $F$  have the same origin and destination coordinates as when the tasks are being performed, the vehicle remains idle (i.e., the EB does not change its physical location while charging or waiting at the depot).

**Table 4.** Coordinates of the task nodes.

Task Node	Origin Location		Destination Location	
	Latitude	Longitude	Latitude	Longitude
$o_1$	677908	6150220	677908	6150220
$o_2$	677908	6150220	677908	6150220
$d_1$	585053	6140355	585053	6140355
$d_2$	720134	6210199	720134	6210199



Table 4. Cont.

Task Node	Origin Location		Destination Location	
	Latitude	Longitude	Latitude	Longitude
1	538181	6086484	720415	6176264
2	538181	6086484	720415	6176264
3	528913	6152557	710831	6168718
4	528913	6152557	710831	6168718
5	538181	6086484	720415	6176264
6	528913	6152557	710831	6168718
1001	557926	6181752	557926	6181752
1002	609023	6077163	609023	6077163
1011	557926	6181752	557926	6181752
1012	609023	6077163	609023	6077163
1021	557926	6181752	557926	6181752
1022	609023	6077163	609023	6077163
1031	557926	6181752	557926	6181752
1032	609023	6077163	609023	6077163
2001	557926	6181752	557926	6181752
2002	609023	6077163	609023	6077163
2011	557926	6181752	557926	6181752
2012	609023	6077163	609023	6077163
2021	557926	6181752	557926	6181752
2022	609023	6077163	609023	6077163
2031	557926	6181752	557926	6181752
2032	609023	6077163	609023	6077163

The Euclidean distances between the nodes were calculated from the depicted coordinates, allowing the travel time  $\tilde{t}_i$  and consumed energy  $\eta_i$  of the trip  $i \in V$  being performed to be computed, presented below in Table 5.

Table 5. Travel time and consumed energy for every performed trip  $i \in V$ .

$i \in V$	$\tilde{t}_i$	$\eta_i$
1	203.1494011	335.1965118
2	203.1494011	335.1965118
3	182.6344344	301.3468168
4	182.6344344	301.3468168
5	203.1494011	335.1965118
6	182.6344344	301.3468168

Table 6 presents the travel times obtained from the end node of event  $i \in N$ , to the initial node of another event  $j \in N$ .

Table 7 presents the energy consumption,  $\theta_{ij}$ , from the end node of event  $i \in N$ , to the start node of another event  $j \in N$ .

Every task node, including that of charging events, was given a time window, as depicted in Table 8.

Notably, the time windows of the multi-port charging events are the same as those assigned to their single-port variant. This is due to the nature of what constitutes as a change in multi-port events. For them to occur, they would have to take place within the same time frame of the two vehicles being at the charging station, so that the change in event can then be registered, should an EV either join or leave.

The additional parameters of the designed toy network were assigned as follows:

- Unit passenger waiting cost of a vehicle:  $\lambda = 1$
- Maximum State of Charge (SOC) of vehicle  $k$  when fully charged:  $\phi_{\max}^k = 1000$
- Minimum SOC permitted to vehicle  $k$ :  $\phi_{\min}^k = 10$
- Travel cost per km = 10

- Consumed energy per minute of the charging rate when 1 port is being occupied:  $r1 = 20$
- Consumed energy per minute of the charging rate when 2 ports are being occupied:  $r2 = 12$
- Energy consumption per km:  $e = 1.65$

**Table 6.** Travel time  $t_{ij}$  between the end location of node  $i \in N$  to the start location of node  $j \in N$  when deadheading.

	$o_1$	$o_2$	$d_1$	$d_2$	1	2	3	4	5	6	1001–1031/ 2001–2031	1002–1032/ 2002–2032
$o_1$	0.00	0.00	93.38	73.35	153.58	153.58	149.01	149.01	153.58	149.01	124.06	100.41
$o_2$	0.00	0.00	93.38	73.35	153.58	153.58	149.01	149.01	153.58	149.01	124.06	100.41
$d_1$ 21	93.38	93.38	0.00	152.07	71.41	71.41	57.45	57.45	71.41	57.45	49.49	67.59
$d_2$	73.35	73.35	152.07	0.00	220.03	220.03	199.72	199.72	220.03	199.72	164.68	173.33
1	49.85	49.85	140.04	33.94	0.00	203.15	192.96	192.96	203.15	192.96	162.58	149.09
2	49.85	49.85	140.04	33.94	203.15	0.00	192.96	192.96	203.15	192.96	162.58	149.09
3	37.76	37.76	128.94	42.51	191.23	191.23	0.00	182.63	191.23	182.63	153.46	136.92
4	37.76	37.76	128.94	42.51	191.23	191.23	182.63	0.00	191.23	182.63	153.46	136.92
5	49.85	49.85	140.04	33.94	203.15	203.15	192.96	192.96	0.00	192.96	162.58	149.09
6	37.76	37.76	128.94	42.51	191.23	191.23	182.63	182.63	191.23	0.00	153.46	136.92
1001–1031/ 2001–2031	124.06	124.06	49.49	164.68	97.29	97.29	41.16	41.16	97.29	41.16	0.00	116.40
1002–1032/ 2002–2032	100.41	100.41	67.59	173.33	71.45	71.45	110.01	110.01	71.45	110.01	116.40	0.00

**Table 7.** Consumed energy  $\theta_{ij}$  from the end location of node  $i \in N$  to the start location of node  $j \in N$  when deadheading.

	$o_1$	$o_2$	$d_1$	$d_2$	1	2	3	4	5	6	1001–1031/ 2001–2031	1002–1032/ 2002–2032
$o_1$	0.00	0.00	154.07	121.03	253.40	253.40	245.87	245.87	253.40	245.87	204.69	165.68
$o_2$	0.00	0.00	154.07	121.03	253.40	253.40	245.87	245.87	253.40	245.87	204.69	165.68
$d_1$	154.07	154.07	0.00	250.91	117.82	117.82	94.79	94.79	117.82	94.79	81.66	111.52
$d_2$	121.03	121.03	250.91	0.00	363.05	363.05	329.54	329.54	363.05	329.54	271.73	286.00
1.00	82.25	82.25	231.07	55.99	0.00	335.20	318.39	318.39	335.20	318.39	268.26	246.01
2.00	82.25	82.25	231.07	55.99	335.20	0.00	318.39	318.39	335.20	318.39	268.26	246.01
3.00	62.31	62.31	212.74	70.14	315.54	315.54	0.00	301.35	315.54	301.35	253.21	225.92
4.00	62.31	62.31	212.74	70.14	315.54	315.54	301.35	0.00	315.54	301.35	253.21	225.92
5.00	82.25	82.25	231.07	55.99	335.20	335.20	318.39	318.39	0.00	318.39	268.26	246.01
6.00	62.31	62.31	212.74	70.14	315.54	315.54	301.35	301.35	315.54	0.00	253.21	225.92
1001–1031/ 2001–2031	204.69	204.69	81.66	271.73	160.53	160.53	67.91	67.91	160.53	67.91	0.00	192.07
1002–1032/ 2002–2032	165.68	165.68	111.52	286.00	117.90	117.90	181.51	181.51	117.90	181.51	192.07	0.00

The MILP was programmed in Python 3.7 and solved through Gurobi using the branch-and-cut and dual simplex methods. The globally optimal solution had an objective function cost of 13340.6 resulting in:

- Vehicle  $k = 1$  serving the task node sequence of:  $o_1 \rightarrow 1 \rightarrow 2011 \rightarrow 4 \rightarrow d_1$ .
- Vehicle  $k = 2$  serving the task node sequence of:  $o_2 \rightarrow 3 \rightarrow 1011 \rightarrow 2 \rightarrow 1031 \rightarrow 6 \rightarrow 1022 \rightarrow 5 \rightarrow d_2$ .

**Table 8.** Time window  $[l_i, u_i]$  for each task node  $i \in N$ .

Task Node	$l_i$	$u_i$
$o_1$	0	20
$o_2$	0	20
$d_1$	800	6000
$d_2$	800	6000
1	20	240
2	420	640
3	40	260
4	440	1060
5	820	2820
6	840	4840
1001/2001	20	270
1011/2011	270	520
1021/2021	520	890
1031/2031	890	1450
1002/2002	800	1000
1012/2012	1000	1250
1022/2022	1250	1500
1032/2032	1500	1800

The route sequence and associated time  $T_i^k$  for which service began at each visiting node  $i \in N$  by vehicle  $k \in K$  is presented below. Table 9 presents the scenario for vehicle 1, and Table 10 for vehicle 2. It should be noted that the depicted service times of the routes are within the upper and lower bounds of the provided time windows. The SOC of each visited task node upon arrival  $e_i^k$ , and upon departure  $\bar{e}_i^k$  are also presented in the second and the third row of the tables. The SOC values are all within the previously mentioned range of  $[\phi_{\min}^k, \phi_{\max}^k] = [10, 1000]$ .

**Table 9.** Time  $T_i^1$  that service begins at each visited node  $i$  of the route of vehicle  $k = 1$ .

Route Sequence of Visited Nodes					
	$o_1$	1	2011	4	$d_1$
$T_i^1$	0	153.6	519.3	631.9	943.4
$e_i^1$	-	746.6	143.1	932.1	418.0
$\bar{e}_i^1$	1000	411.4	1000	630.7	-

**Table 10.** Time  $T_i^2$  that service begins at each visited node  $i$  of the route of vehicle  $k = 2$ .

Route Sequence of Visited Nodes									
	$o_2$	3	1011	2	1031	6	1022	5	$d_2$
$T_i^2$	17.6	166.6	502.7	640.0	1005.7	1085.1	1404.6	1525.7	1762.8
$e_i^2$	-	754.1	1000	893.5	236.0	932.1	404.8	882.1	490.9
$\bar{e}_i^2$	1000	452.8	1000	504.3	1000	630.7	1000	546.9	-

From the routes of the two vehicles, the potential for multi-port charging can be observed for charging events  $i = 2011$  of vehicle  $k = 1$ , and  $i = 1011$  of  $k = 2$ , both indexed at the same charging station  $z = 1$  and at the same charging interval  $[270-520]$ . Vehicle 1 arrives after vehicle 2 within the *same charging time interval* and it uses the second port of the charging station. These two charging events at the two ports of the charging station fall within the same time window of  $[l_i, u_i] = [270, 520]$ , with an arrival time difference of  $519.3 - 502.7 = 16.6$ .

Vehicle 1 charges only at the first charging station using its second charging port ( $i = 2011$ ). Vehicle 2 charges three times in total. Two times at the first charging station

( $i = 1011$  and  $i = 1031$ ), and one time at the second charging station ( $i = 1022$ ). During its first charge at the first charging station, vehicle 2 shares the charging station with vehicle 1. During its second and third charging, vehicle 2 charges alone at the respective charging station.

It is additionally worth noting that for the generated routes, the first electric bus performs two trips (1 and 4), and the second electric bus performs four trips (3, 2, 6 and 5). To highlight the importance of the multi-port formulation, the same example cannot be solved if we consider that each one of the two charging stations has a single port, as such a problem is found to possess *no feasible solution*. This means that the bus operator would need an extra third bus to perform the six scheduled trips on time. This underlines the benefit of using multiple ports: although the charging rate in a charging station decreases when multiple buses are charging at the same time, this charging time increase might still suffice for the scheduled trips to be performed, without the need for deploying additional buses.

## 5. Computational Results

### 5.1. Experiments

Computational experiments of larger instances were performed to analyze the complexity of the presented framework. A set of EB-MDVSPWTW benchmark instances from Gkiotsalitis et al. [30] were appropriated into two-port variants and used to test our multi-port EB-MDVSPWTW model. All the depots, charging stations, starting, and ending points of the trip nodes followed a uniform distribution within a 60 km by 60 km square Euclidean plane. For each scenario, a vehicle drives 60 km in 1 h, as the inter-node travel times (measured in minutes) are directly equivalent to the Euclidean distance between the nodes. No restrictions were applied to the trip/depot combinations. For comparative purposes, the necessary parameters were directly adapted from the 10-trip test instance each benchmark test-dataset was based on. This includes the number of vehicles (2), number of trips (10), waiting time cost (2), maximum SOC (300), minimum SOC (10), travel time cost (10) and energy consumption per kilometer (1.3). The rate of charge was modified into a vector of two variables such that the single-port charging rate was set to 20, and the double-port charging rate was set to 12. The same time windows and coordinate system of each corresponding task node and charging station was maintained.

Two classes of instances are displayed in Table 11. For each class, the total number of trips, depots, charging stations and generated instances are listed. The 10-trip instances of varied charging stations were solved by Gurobi 10.0.0 using branch-and-cut and dual simplex. The numerical experiments were executed on a conventional Intel(R) Core (TM) i3-1005G1 CPU @ 1.20 GHz CPU model. The criterion for termination of the solver was the convergence to a globally optimal solution.

**Table 11.** Multi-port EB-MDVSPWTW instances.

Name	Vehicles	Depots	Chargers	Charging Events	Trips	Instances
Z2_S2_C10	2	2	2	16	10	5
Z2_S4_C10	2	2	4	16	10	5

The results for the 10-trip instances Z2\_S2\_C10 and Z2\_S4\_C10 are shown in Table 12. For each instance, the number of nodes explored in the rooted tree (NE), the number of simplex iterations (SI), the computational time (CT) in seconds, the solution performance (SP) and the optimality gap (OG) are presented.

In these computational results, the emphasis is placed on computational performance. As it can be observed, networks with four charging stations, two ports per station and ten trips might require more than 1 h to solve to global optimality using a conventional computing machine. Although the above experiments cannot run for single-port instances because we have structured the input data in a multi-port format, we ran experiments in benchmark instances with similar size to compare the number of evaluated B&B nodes,

the simplex iterations, and the computation times. The computational results of solving single-port instances are presented in Table 13.

**Table 12.** Ten-trip instances results for multiple ports. NE: B&B Nodes Evaluated; SI: Simplex Iterations; CT: Computation Time in seconds; SP: Solution Performance; OG: Optimality Gap.

Instance	NE	SI	CT	SP	OG
Z2_S2_C10_a_TW	62,330	3,356,341	466.32	1909.32	0.00%
Z2_S2_C10_b_TW	65,155	2,793,402	378.10	1478.27	0.00%
Z2_S2_C10_c_TW	619,050	22,154,420	2616.78	2285.58	0.00%
Z2_S2_C10_d_TW	27,036	1,472,061	381.74	1338.73	0.00%
Z2_S2_C10_e_TW	47,105	2,346,572	315.92	1774.88	0.00%
Z2_S4_C10_a_TW	890,447	43,358,868	4322.69	2355.38	0.00%
Z2_S4_C10_b_TW	247,506	11,662,307	1121.65	1661.05	0.00%
Z2_S4_C10_c_TW	48,495	2,782,933	547.73	2008.26	0.00%
Z2_S4_C10_d_TW	309,489	16,498,932	1620.39	1722.26	0.00%
Z2_S4_C10_e_TW	132,464	5,553,343	670.89	2116.74	0.00%
Averages	244,908	11,197,918	1244.22		

**Table 13.** Ten-trip instances results for single ports. NE: B&B Nodes Evaluated; SI: Simplex Iterations; CT: Computation Time in seconds; OG: Optimality Gap.

Instance	NE	SI	CT	OG
D2_S2_C10_a	21,859	1,063,498	147.33	0.00%
D2_S2_C10_b	15,139	824,897	117.33	0.00%
D2_S2_C10_c	43,498	1,726,351	166.09	0.00%
D2_S2_C10_d	20,172	977,038	133.52	0.00%
D2_S2_C10_e	23,312	1,087,117	152.66	0.00%
D2_S4_C10_a	22,681	1,061,138	152.91	0.00%
D2_S4_C10_b	34,904	1,358,652	137	0.00%
D2_S4_C10_c	20,909	1,137,567	153.18	0.00%
D2_S4_C10_d	14,731	755,716	83.71	0.00%
D2_S4_C10_e	18,582	863,815	141.73	0.00%
Averages	23,578.7	1,085,579	51.56	
Difference in averages between single- and multi-port problems	938.68%	931.52%	2313.06%	

In the last row of Table 13, one can observe the average computation time differences between the single-port and the multi-port problems when using the same computer machine in instances with similar sizes. In terms of average nodes explored, there was an increase of 938.683% when the problem involved multiple ports. The multi-port approach also increased the number of required simplex iterations by 931.52%. The increased complexity is further corroborated by the 2313.06% rise in average computation times. This suggests that the multi-port EB-VSP problem is considerably more computationally expensive compared to the single-port EB-VSP problem. This is in line with expectations, considering the sizable dependence computational performance has on input data. The examined two-port approach presented in this paper possesses twice the number of charging event task nodes that require processing, naturally providing more input to be computed. Lastly, it must be noted that the changes in computational performances of the ten benchmark instances have consistently increased among all performance markers.

## 5.2. Limitations

Here, we present the limitations of our study with respect to the implementation of multi-port charging stations. First, multi-port charging stations can overheat if too many vehicles are charging at once. This can cause damage to the charging station and the vehicles. Overheating can also be a fire hazard, therefore one should ensure that the



multi-port charging station is placed in a well-ventilated area. Second, as detailed in the formulation of our study, multi-port charging stations can result in slower charging speeds compared to the single-port alternatives. Third, even though multi-port charging stations can result in lower costs in the long run, they may be more expensive to purchase compared to single-port alternatives.

Regarding the implementation of our model, it is necessary to consider the limitations in testing our model on a toy network. The Euclidean calculations depicting the distances between the simulated nodes of the problem instances were used for demonstration purposes and they should be replaced by shortest path distances in real-world settings. Furthermore, the demonstrations were conducted within the problem setting of two ports. Future research can consider testing scenarios with charging stations having three or more ports. Lastly, the computational experiments used instances of up to ten trips. In future research, more vehicle trips can be considered.

## 6. Conclusions

The design of charging stations for bus operations has become a field of significant interest. The addition of multiple ports to a fixed charging station is primed as a sustainable approach for using existing infrastructure to support improved electromobility operations.

This study set out to adapt the existing EB-MDVSPTW to account for fixed multi-port charging stations. The new formulation was presented and examined using two vehicle networks of various sizes and scenarios. Test instances (including both a toy network and benchmark instances of the original EB-MDVSPTW) were used to explore the performance of the multi-port formulation. In the toy network, the multi-port formulation was able to provide a solution with the use of two electric buses, whereas the single-port formulation required an extra bus to perform the required bus trips.

Within the scope of computational complexity, Desrosiers et al. [32] showed that problem complexity grows along with the width of assigned time windows, further supporting the necessity for specifically investigating significantly reduced time window variations. The testing of the ten benchmark instances shed light on the computational performance of the solution framework. Largely dependent on input data, the doubling of the processed task nodes when considering multiple ports was found to significantly impact the computational processing and efficiency. In particular, the CPU time increased considerably compared to the case of solving the single-port EB-MDVSPTW problem.

Given the above, when solving for the multi-port EB-MDVSPTW problem, a heavy computational workload must be accounted for, either by using parallel computing or (meta)heuristic approaches that can provide suboptimal solutions for larger instances. While exact methods guarantee optimality, they tend to come at the cost of prolonged processing time. Alternative methodologies like metaheuristics may thus be considered. For the real-world testing of the multi-port model, shortest path or pre-defined route distances can be considered, instead of the Euclidean distances employed for the toy network demonstration. Additionally, real-time considerations (for, e.g., a framework capable of streamlining real-time data input and an adapted methodology capable of the dynamic computation), suited for operationalizing the modeling approach presented in this paper, may be investigated in future research. Within the scope of sustainability, the extension of the presented model by considering the use of renewable energy can be considered for further investigation. In this direction, unique considerations (i.e., emission reduction goals or geographical factors affecting the availability of solar or wind energy) may need to be factored into the mathematical formulation in terms of modeling constraints. In terms of potential applications, our approach can be applied in charging networks with space and grid capacity limitations, where the use of multiple ports can enable the charging of multiple vehicles at once.

**Author Contributions:** Conceptualization, K.G., M.L.Y.C. and D.K.; methodology, K.G., M.L.Y.C. and D.K.; software, M.L.Y.C. and D.K.; validation, M.L.Y.C. and D.K.; formal analysis, M.L.Y.C. and D.K.; investigation, K.G., M.L.Y.C. and D.K.; data curation, M.L.Y.C. and D.K.; writing—original

draft preparation, M.L.Y.C. and D.K.; writing—review and editing, K.G.; supervision, K.G.; funding acquisition, K.G. All authors have read and agreed to the published version of the manuscript.

**Funding:** This research received no external funding.

**Institutional Review Board Statement:** Not applicable.

**Informed Consent Statement:** Not applicable.

**Data Availability Statement:** The data presented in this study are available on request from the corresponding author.

**Conflicts of Interest:** The authors declare no conflict of interest.

## References

- Mathiesen, B.V.; Ilieva, L.S.; Skov, I.R.; Maya-Drysdale, D.W.; Korberg, A.D. *REPowerEU and Fitfor55 Science-Based Policy Recommendations for Achieving the Energy Efficiency First Principle*; Report, 2022; Aalborg University: Copenhagen, Denmark, 2022.
- Rietmann, N.; Hügler, B.; Lieven, T. Forecasting the trajectory of electric vehicle sales and the consequences for worldwide CO<sub>2</sub> emissions. *J. Clean. Prod.* **2020**, *261*, 121038. [\[CrossRef\]](#)
- Eudy, L.; Caton, M.; Post, M.; National Renewable Energy Laboratory (NREL) (U.S.). *Transit Investments for Greenhouse Gas and Energy Reduction Program: Second Assessment Report*; Technical Report FTA Report No. 0064; Federal Transit Administration—Office of Research, Demonstration, and Innovation: Washington, DC, USA, 2014. [\[CrossRef\]](#)
- Mahmoud, M.; Garnett, R.; Ferguson, M.; Kanaroglou, P. Electric buses: A review of alternative powertrains. *Renew. Sustain. Energy Rev.* **2016**, *62*, 673–684. [\[CrossRef\]](#)
- Lajunen, A.; Lipman, T. Lifecycle cost assessment and carbon dioxide emissions of diesel, natural gas, hybrid electric, fuel cell hybrid and electric transit buses. *Energy* **2016**, *106*, 329–342. [\[CrossRef\]](#)
- Neff, J.; Dickens, M. 2016 *Public Transportation Fact Book*; American Public Transportation Association: Washington, DC, USA, 2008.
- Acumen Research and Consulting. Electric Bus Market to Grow Significantly at 26.1% of CAGR by 2026. 2020. Available online: <https://www.globenewswire.com/news-release/2020/03/12/1999947/0/en/Electric-Bus-Market-to-Grow-Significantly-at-26-1-of-CAGR-by-2026.html> (accessed on 15 December 2023).
- Wu, W.; Lin, Y.; Liu, R.; Jin, W. The multi-depot electric vehicle scheduling problem with power grid characteristics. *Transp. Res. Part B Methodol.* **2022**, *155*, 322–347. [\[CrossRef\]](#)
- Iliopoulou, C.; Tassopoulos, I.; Kepaptsoglou, K.; Beligiannis, G. Electric Transit Route Network Design Problem: Model and Application. *Transp. Res. Rec.* **2019**, *2673*, 264–274.
- Fuller, M. Wireless charging in California: Range, recharge, and vehicle electrification. *Transp. Res. Part C Emerg. Technol.* **2016**, *67*, 343–356. [\[CrossRef\]](#)
- Perumal, S.S.G.; Lusby, R.M.; Larsen, J. Electric bus planning & scheduling: A review of related problems and methodologies. *Eur. J. Oper. Res.* **2022**, *301*, 395–413. [\[CrossRef\]](#)
- Zhu, Z.H.; Gao, Z.Y.; Zheng, J.F.; Du, H.M. Charging station location problem of plug-in electric vehicles. *J. Transp. Geogr.* **2016**, *52*, 11–22. [\[CrossRef\]](#)
- Mukherjee, B.; Sossan, F. Optimal Planning of Single-Port and Multi-Port Charging Stations for Electric Vehicles in Medium Voltage Distribution Networks. *arXiv* **2021**, arXiv:2111.07100.
- Wang, C.N.; Yang, F.C.; Vo, N.T.M.; Nguyen, V.T.T. Enhancing Lithium-Ion Battery Manufacturing Efficiency: A Comparative Analysis Using DEA Malmquist and Epsilon-Based Measures. *Batteries* **2023**, *9*, 317. [\[CrossRef\]](#)
- Bai, H.; Fan, Y.; Wang, L.; Vo, N.; Nguyen, T. Research on Battery Characteristics and Management System of New Energy Vehicle Based on BMS System Design and Test. *Comput. Aided Des. Appl.* **2022**, *20*, 200–212. [\[CrossRef\]](#)
- Gao, Z.; Lin, Z.; LaClair, T.J.; Liu, C.; Li, J.M.; Birky, A.K.; Ward, J. Battery capacity and recharging needs for electric buses in city transit service. *Energy* **2017**, *122*, 588–600. [\[CrossRef\]](#)
- Wen, M.; Linde, E.; Ropke, S.; Mirchandani, P.; Larsen, A. An adaptive large neighborhood search heuristic for the Electric Vehicle Scheduling Problem. *Comput. Oper. Res.* **2016**, *76*, 73–83. [\[CrossRef\]](#)
- Sassi, O.; Oulamara, A. Electric vehicle scheduling and optimal charging problem: Complexity, exact and heuristic approaches. *Int. J. Prod. Res.* **2017**, *55*, 519–535. [\[CrossRef\]](#)
- Gkiotsalitis, K. *Public Transport Optimization*; Springer Nature: Berlin/Heidelberg, Germany, 2023.
- Adler, J.D. *Routing and Scheduling of Electric and Alternative-Fuel Vehicles*; Technical report; Arizona State University: Tempe, AZ, USA, 2014.
- Rogge, M.; van der Hurk, E.; Larsen, A.; Sauer, D.U. Electric bus fleet size and mix problem with optimization of charging infrastructure. *Appl. Energy* **2018**, *211*, 282–295. [\[CrossRef\]](#)
- Wang, Y.; Huang, Y.; Xu, J.; Barclay, N. Optimal recharging scheduling for urban electric buses: A case study in Davis. *Transp. Res. Part E Logist. Transp. Rev.* **2017**, *100*, 115–132. [\[CrossRef\]](#)

23. Jiang, M.; Zhang, Y.; Zhang, Y.; Zhang, C.; Zhang, K.; Zhang, G.; Zhao, Z. Operation and Scheduling of Pure Electric Buses under Regular Charging Mode. In Proceedings of the 2018 21st International Conference on Intelligent Transportation Systems (ITSC), Maui, HI, USA, 4–7 November 2018; pp. 1894–1899. [\[CrossRef\]](#)
24. Yao, E.; Liu, T.; Lu, T.; Yang, Y. Optimization of electric vehicle scheduling with multiple vehicle types in public transport. *Sustain. Cities Soc.* **2020**, *52*, 101862. [\[CrossRef\]](#)
25. Li, X.; Wang, T.; Li, L.; Feng, F.; Wang, W.; Cheng, C. Joint Optimization of Regular Charging Electric Bus Transit Network Schedule and Stationary Charger Deployment considering Partial Charging Policy and Time-of-Use Electricity Prices. *J. Adv. Transp.* **2020**, *2020*, 8863905. [\[CrossRef\]](#)
26. Liu, T.; Ceder, A.A. Battery-electric transit vehicle scheduling with optimal number of stationary chargers. *Transp. Res. Part C Emerg. Technol.* **2020**, *114*, 118–139. [\[CrossRef\]](#)
27. Zhang, L.; Liu, Z.; Wang, W.; Yu, B. Long-term charging infrastructure deployment and bus fleet transition considering seasonal differences. *Transp. Res. Part D Transp. Environ.* **2022**, *111*, 103429. [\[CrossRef\]](#)
28. Montoya, A.; Guéret, C.; Mendoza, J.E.; Villegas, J.G. The electric vehicle routing problem with nonlinear charging function. *Transp. Res. Part B Methodol.* **2017**, *103*, 87–110. [\[CrossRef\]](#)
29. Felipe, Á.; Ortuño, M.T.; Righini, G.; Tirado, G. A heuristic approach for the green vehicle routing problem with multiple technologies and partial recharges. *Transp. Res. Part E Logist. Transp. Rev.* **2014**, *71*, 111–128. [\[CrossRef\]](#)
30. Gkiotsalitis, K.; Iliopoulou, C.; Kepaptsoglou, K. An exact approach for the multi-depot electric bus scheduling problem with time windows. *Eur. J. Oper. Res.* **2023**, *306*, 189–206. [\[CrossRef\]](#)
31. Barraza, O.; Estrada, M. Battery electric bus network: Efficient design and cost comparison of different powertrains. *Sustainability* **2021**, *13*, 4745. [\[CrossRef\]](#)
32. Desrosiers, J.; Dumas, Y.; Solomon, M.; Soumis, F. Time Constrained Routing and Scheduling. *Handbooks Oper. Res. Manag. Sci.* **1995**, *8*, 35–139. [\[CrossRef\]](#)

**Disclaimer/Publisher’s Note:** The statements, opinions and data contained in all publications are solely those of the individual author(s) and contributor(s) and not of MDPI and/or the editor(s). MDPI and/or the editor(s) disclaim responsibility for any injury to people or property resulting from any ideas, methods, instructions or products referred to in the content.